

# The CFD Computation and Validation of Effects of Adaptive Mesh Refinement in Sloshing Simulation in A Narrow Tank

Emre Sayak<sup>1</sup>, Sıtkı Uslu<sup>1</sup>

<sup>1</sup>TOBB University of Economy and Technology University Söğütözü, Söğütözü Cd. No:43, 06510 Çankaya/Ankara  
e.sayak@etu.edu.tr, suslu@etu.edu.tr

**Abstract** – Strong and precise computational methods are necessary to discover and understand undesirable effects in tanks where liquids slosh, known as sloshing. Sloshing is important for many industrial applications, such as fuel tanks in ships, aircraft, and other transport vehicles. Numerical methods are commonly used in modelling sloshing behaviour, and adaptive mesh refinement (AMR) technology is an effective method used to increase numerical accuracy in sloshing simulations. The primary objective of this research is to conduct Computational Fluid Dynamics (CFD) calculations of sloshing phenomena to establish a methodology for observing the undesirable effects on the relevant system and assess the effectiveness of adaptive mesh refinement by comparing the results of surface impact pressures with experimental case results from literature. A 3D model of a rectangular tank partially filled with water is used to simulate the impact pressure caused by roll motion. The roll motion is based on experimental data and occurs at periods close to the tank's internal wave resonance period. The pressure results are observed from a single monitoring point. Numerical studies are performed using Star CCM+ software. The Volume of Fluid (VOF) based Eulerian method is utilised to model the free surface flow. The study demonstrates the ability of AMR to accurately model sloshing behaviour and compares fixed and AMR grids at different levels. Finally, the results of fixed and adaptive cartesian grids are compared and verified with corresponding experimental data. The results showed that the AMR grid provided higher numerical accuracy, lower computational cost and allowed for more accurate modelling of sloshing behaviour. It is emphasised that the importance of AMR for understanding sloshing behaviour and modelling it accurately.

**Keywords:** sloshing, free surface flow, adaptive mesh refinement, multiphase flow, volume of fluid

## 1. Introduction

To define sloshing, it refers to the movement or oscillation of a liquid free surface inside a container that is subjected to external disturbances such as roll or pitch motion. The sloshing phenomenon can lead to undesired effects, such as performance and stability reduction or structural damage, and it is, therefore, important to accurately predict and understand the sloshing behaviour in order to design and operate various types of systems safely and efficiently. Sloshing should be considered for any moving structure or vehicle transporting liquid. Therefore, numerous researchers have been working on the problem of sloshing for many years. Researchers have explored this problem using a variety of methods, including analytical, numerical, and experimental techniques [1].

The earliest known studies on the movement of liquids date back to Euler's research in 1761 [2]. Since then, this phenomenon is important for many industrial applications, such as fuel tanks in ships, aircraft, and other transport vehicles. Hence, several analytical and approximate methods for predicting sloshing motion have been proposed [3-5]. However, solving this mathematical problem analytically is challenging due to the nonlinearity of the dynamic boundary condition at the free surface and the unpredictable time variation of the free surface position. Numerical models and experimental studies have been developed to model sloshing accurately in partially filled tanks through the analysis of surface impact pressures. Experimental studies are necessary to confirm theoretical and computational investigations. Several experimental studies have proposed aimed to investigate sloshing effects and impact pressures [6-10]. Sloshing analysis is a complex problem that requires both experimental and numerical investigations to obtain accurate results. While numerical models provide a cost-effective and efficient way of predicting the behaviour of sloshing fluids, they need to be validated against experimental data to ensure their accuracy. On the other hand, experimental studies alone may not be sufficient to provide a complete understanding of sloshing dynamics and may be limited by the availability of appropriate testing facilities and equipment. Therefore, a combined approach that utilises both experimental and numerical methods can provide a comprehensive and

reliable analysis of sloshing phenomena. In recent years, computational fluid dynamics (CFD) has become a valuable tool for simulating sloshing behaviour and predicting the impact of sloshing on tanks and their support structures. CFD simulations can provide insights into the complex fluid-structure interactions and enable optimization of the design of the tank and its support structure. One of the challenges in CFD simulations is the trade-off between the computational cost and accuracy of the simulation results. It is worth noting that adaptive mesh refinement has been studied in the literature for sloshing simulations. These studies present numerical models for simulating two-phase flow, utilizing adaptive mesh refinement for efficient resolution of the computational domain. Different types of adaptive mesh schemes have been developed and investigated according to the free surface behaviour. The results are verified with experiments [11-13]. The mesh resolution plays a critical role in determining the accuracy of the simulation results, but finer meshes can significantly increase the computational cost. Adaptive Mesh Refinement (AMR) is a promising method to address this challenge by refining the mesh in regions of interest while maintaining a coarser mesh in other regions.

In this paper, it is presented a study on the effects of AMR on sloshing simulations in partially filled narrow span rectangular tank. The capability of different levels of AMR to accurately replicate sloshing behaviour is investigated, and the results are compared with fixed grid simulations. The numerical outcomes of different levels of adaptive cartesian grids and fixed cartesian grid cases are compared and verified using experimental data. The results show that AMR can significantly improve the accuracy of sloshing simulations while reducing the computational cost. This study provides insights into the use of AMR in sloshing simulations and its potential for improving the design and operation of liquid- carrying structures and vehicles.

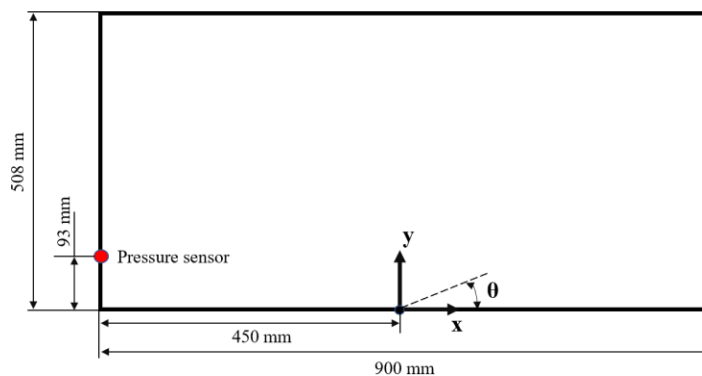
## 2. Experimental and Simulation Model Description

This section describes one of the wave impact experiments conducted by Antonio et al. [10] and used for validation analyses. The lateral impact with water test case was considered for the validation analysis, and the properties of the liquid phase are presented in **Table 1**.

**Table 1.** Liquid phase properties

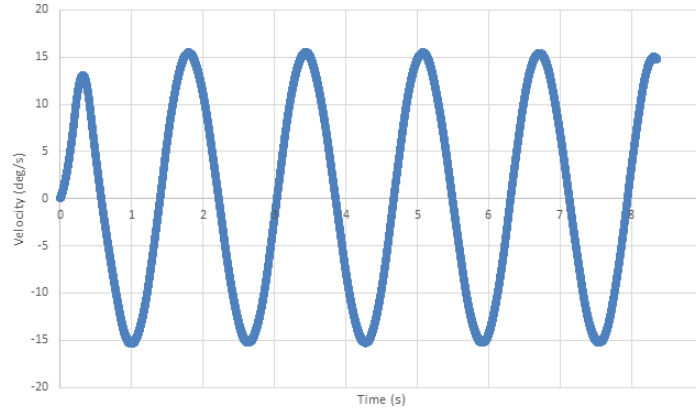
	Density (kg/m <sup>3</sup> )	Dynamic viscosity (Pa.s)	Surface tension (N/m)
Water	998	0.0010	0.0728

Time histories of pressure recorded at a specific location, along with the corresponding roll angle history of the periodic angular motion of the sloshing tank, are also provided. The dimensions of the narrow span rectangular tank and the position of the pressure sensor are shown in Figure 1, and the liquid level for the lateral impact is 93 mm. The other part of the tank is filled with air, and there are no gas or liquid inlets into the system.



**Figure 1.** 2D schematic of the tank dimensions and sensor position

The periodic angular motion history according to the tank axis system can be seen in Figure 2.

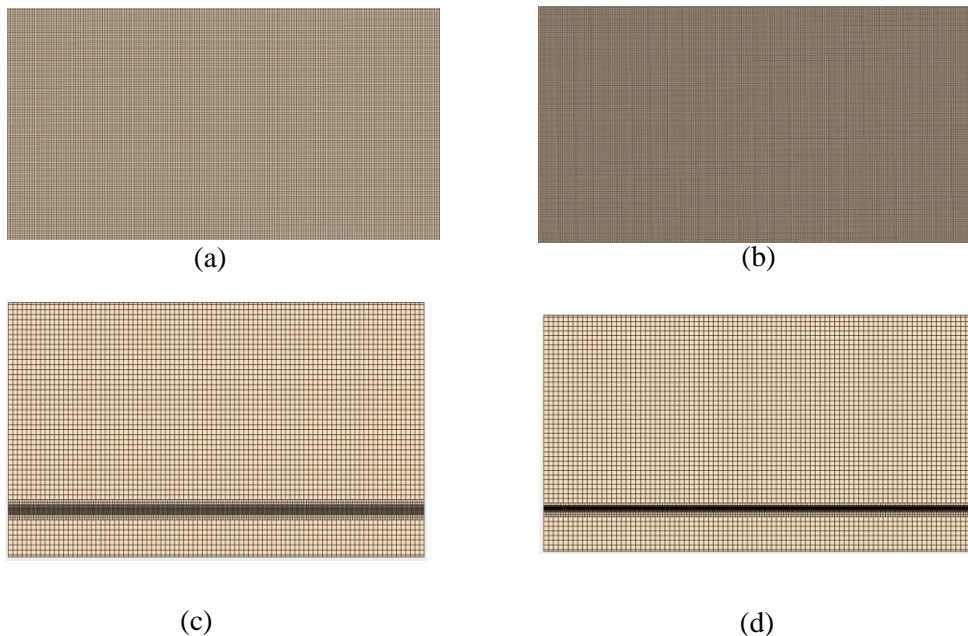


**Figure 2.** Periodic angular motion of the tank

The narrow tank geometry and motion properties from experimental case have been transferred to the simulation. Table 2 provides a summary of the mesh structure characteristics, including the number of mesh elements, aspect ratios, and skewness, which are indicators of mesh quality. The different levels of adaptive cartesian grids and fixed grids can be seen in Figure 3.

**Table 2.** Mesh information of different grids

	Refinement level	Mesh type	Number of elements
Fixed grid-1	-	Trim	308k
Fixed grid-2	-	Trim	857k
Adaptive grid-1	2	Trim	630k
Adaptive grid-2	4	Trim	1.7M



**Figure 3.** Grid structures of a) Fixed grid-1 b) Fixed grid-2 c) Adaptive grid-1 d) Adaptive grid-2

### 3. Mathematical Modelling

There exist various techniques for tracking immiscible interfaces [14]:

- Moving grid or Lagrangian approach (capturing),
- Fixed grid or Eulerian approach (tracking),
- Combined method of Lagrangian and Eulerian for tracking immiscible interfaces.

This research utilizes the VOF method within STAR CCM+, which is a part of the Eulerian approach and multiphase model specifically designed to simulate the flow of multiple immiscible fluids on numerical grids that can resolve the interface between the different phases of the mixture. The modelling approach assumes that the mesh resolution is adequate to determine the position and shape of the interface between the phases. The volume fractions of different phases are calculated differently based on the number of VOF phases present.

For two VOF phases, only the first phase is solved for, and the second phase volume fraction is adjusted to ensure a total sum of 1. For three or more phases, volume fraction transport is solved for each phase and normalized based on the total sum of all phase volume fractions. The dynamics of the m-th fluid in a system consisting of n fluids is described by the transport equation below where  $C_m$  is the volume fraction representing the fraction of a m-th fluid phase in computational cell, and  $\mathbf{U}$  is the fluid velocity vector.

$$\frac{\partial C_m}{\partial t} + \nabla \cdot (C_m \mathbf{U}) = 0 \quad (1)$$

For n phases the constraint can be seen below:

$$\sum_{m=1}^n C_m = 1 \quad (2)$$

For each cell, physical properties such as density  $\rho$  can be seen below:

$$\rho = \sum_{m=1}^n \rho_m C_m \quad (3)$$

The equation below is used to calculate the first sloshing period for a specific depth. Here, "g" represents the acceleration due to gravity, "L" represents the length of the tank, and "H" represents the filling level of the water [10]:

$$T_0 = 2\pi \left( \sqrt{\frac{\pi g}{L} \left( 1 - \tanh\left(\frac{\pi H}{L}\right) \right)} \right)^{-1} \quad (4)$$

No heat transfer calculations were performed in the simulations, and the working fluid pair and ambient temperature were set to 293.16 K. The flow demonstrates turbulent behaviour, characterized by a Reynolds number of 97546 and the turbulence model chosen for the analysis is the realizable k-ε model. The liquid phase is modelled as constant density. In order to obtain a more accurate pressure values resulting from the impact of the liquid on the wall and the entrapped air between the liquid and the wall during sloshing, the gas phase has been modelled as an ideal gas in the simulations. The simulations are time-dependent, and first order implicit unsteady scheme is used to deal with time derivative terms. Numerical schemes of the validation simulations can be seen in Table 3. In the absence of experimental data from tests [10], the validation of different levels of adaptive cartesian grids through VOF equations in CFD can provide evidence that the modelling approach is suitable for validating the numerical model.

**Table 3.** Numerical schemes of simulations

Turbulence model	Liquid phase	Gas phase	Multiphase model	Discretization type
Realizable k- $\epsilon$	Constant density	Ideal gas	VOF	Implicit unsteady

#### 4. CFD Results

The first sloshing impact for the experimental case is determined using Equation 4, resulting in a calculated value of 1.92 seconds. Table 4 presents the motion of the free surface during periodic angular motion for various adaptive and fixed grids within a time interval ranging from 0 to 8.35 seconds. The first impact is observed at 2.4 seconds, and subsequent impacts are identified with a time step of 1.63 seconds ( $0.85T_0$ ), which represents the oscillation period for the experimental case. The obtained results are compared with experimental visual observations. In the figures, the scalar field scenes correspond to the volume fraction of water.

**Table 4.** Movement of the free surface at different times




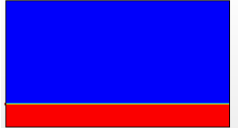
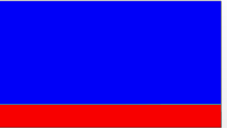

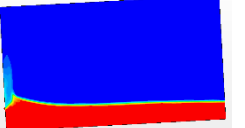
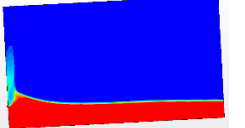



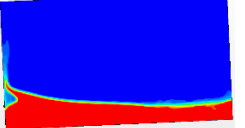
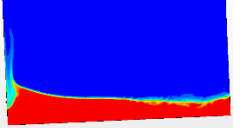
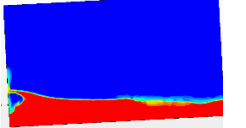

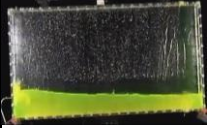
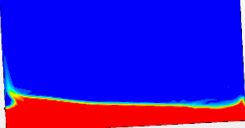
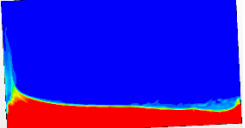
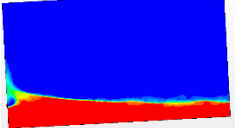
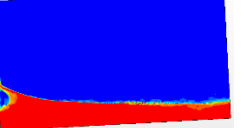
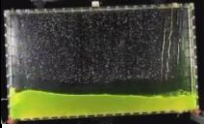
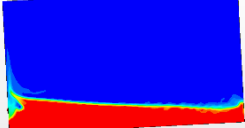
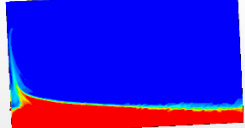
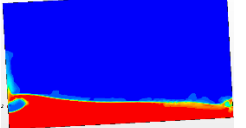
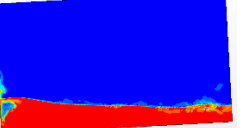
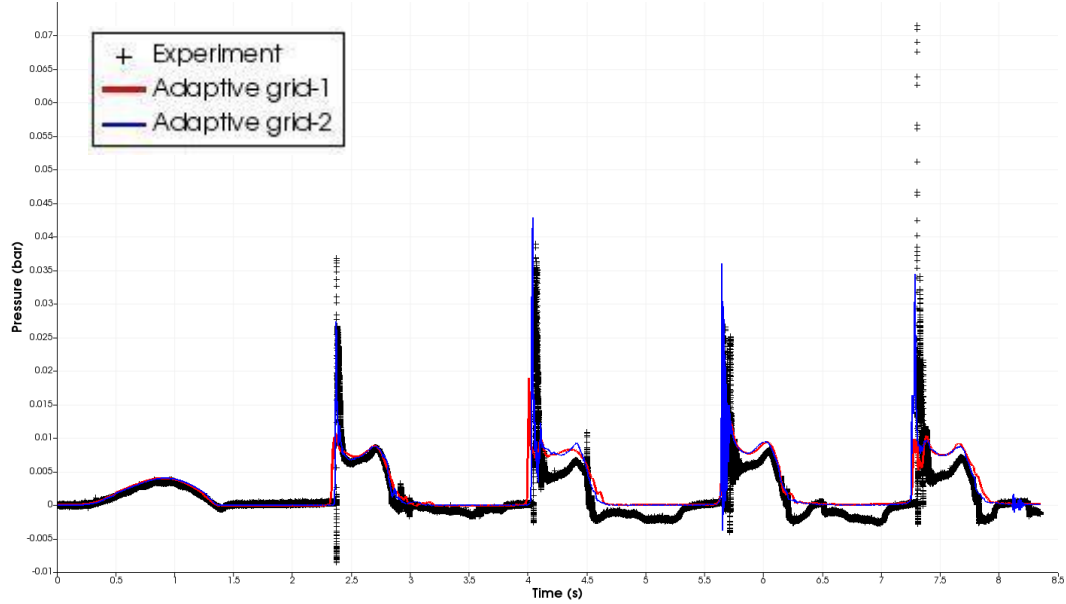
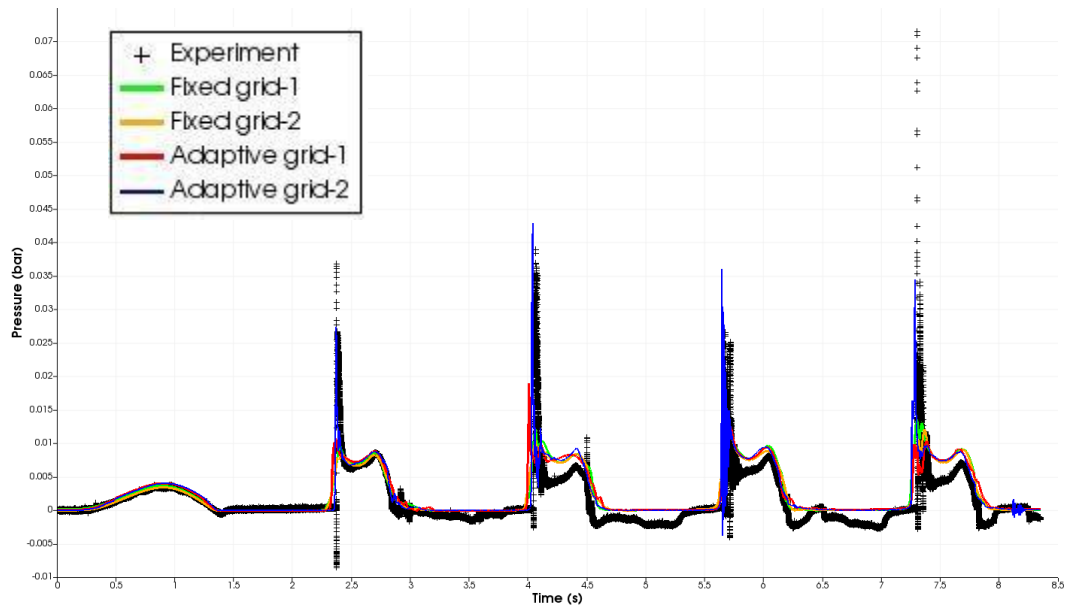
T (s)	Experiment	Fixed grid-1	Fixed grid-2	Adaptive grid-1	Adaptive grid-2
0.00					
2.40					
4.03					
5.66					
7.29					

Figure 4 presents the effects of adaptive refinement level on pressure histories at pressure sensor location with the comparison of experimental results.



**Figure 4.** Pressure results of adaptive grids

Figure 5 presents the comparison of adaptive cartesian grid and fixed cartesian grid pressure history results and the comparison of experimental results.



**Figure 5.** Pressure results of adaptive and fixed grids compared to experimental results

It can be seen that all grids exhibit excellent consistency in terms of the timing of the pressure peak occurrences. According to the graphs, the pressures following the peaks consistently exhibit an overestimation in the simulations. This overestimation of the pressures may be attributed to the inadequate consideration of compressibility effects in the gas phase.

Also, fixed grids have proven to be insufficient in predicting the pressure peak values accurately. The adaptive grid model with four refinement levels has been successful in capturing pressure peak values accurately. **Table 5** shows the simulation run times of the adaptive and fixed grids.

**Table 5.** Simulation run times

	<b>Time (h)</b>
Fixed grid-1	1.78
Fixed grid-2	7.59
Adaptive grid-1	1.84
Adaptive grid-2	25.3

## 5. Conclusion

Adaptive and fixed grid structures were simulated numerically using the commercial CFD code STAR CCM+. The simulations successfully predicted the timing of the pressure peaks. However, the pressure values immediately following the peaks were overestimated, indicating potential limitations in modelling the compressibility effects in the gas phase. While fixed grids are insufficient in capturing pressure peak points, adaptive grids, particularly those with four refinement levels, have been successful in capturing pressure peak values. Nevertheless, upon examining the simulation durations, it is observed that the computational cost of the adaptive grid with four refinement levels is significantly high. At this point, although it may not accurately determine the pressure peak values, using an adaptive grid with two refinement levels could be a reasonable choice in terms of computational cost.

## Acknowledgements

We would like to acknowledge the financial support provided by Roketsan Roket Sanayii ve Ticaret A.S. and TOBB University of Economy and Technology. Our gratitude also extends to Alper Ataseven from IOG Engineering for his valuable assistance throughout the research process.

## References

- [1] R. A. Ibrahim, *Liquid sloshing dynamics: Theory and applications*. Cambridge: Cambridge University Press, 2006.
- [2] Euler, L., 1761. *Principia motus fluidorum*. *Novi Commentarii Acad. Sci. Petropolitanae*, 6(1756/7): p. 271-311.
- [3] W. M. Park et al., "Simple analytical method for predicting the sloshing motion in a rectangular pool," *Nuclear Engineering and Technology*, vol. 52, no. 5, pp. 947–955, 2020.
- [4] O.-M. Balas, C. V. Doicin, and E. C. Cipu, "Analytical and numerical model of sloshing in a rectangular tank subjected to a braking," *Mathematics*, vol. 11, no. 4, p. 949, 2023.
- [5] Kim, J.K., H.M. Koh, and I.J. Kwahk, 1996. Dynamic response of rectangular flexible fluid containers. *Journal of Engineering Mechanics*, 122(9): p. 807-817.
- [6] Akyıldız, H., N.E. Ünal, and H. Aksoy, 2013. An experimental investigation of the effects of the ring baffles on liquid sloshing in a rigid cylindrical tank. *Ocean Engineering*, 59: p. 190-197.
- [7] D. Lu, X. Zeng, J. Dang, and Y. Liu, "A calculation method for the sloshing impact pressure imposed on the roof of a passive water storage tank of AP1000," *Science and Technology of Nuclear Installations*, vol. 2016, pp. 1–8, 2016.
- [8] W. Wu et al., "Experimental study on characteristic of sloshing impact load in elastic tank with low and partial filling under rolling coupled pitching," *International Journal of Naval Architecture and Ocean Engineering*, vol. 12, pp. 178–183, 2020.
- [9] Y.-M. Yu, N. Ma, S.-M. Fan, and X.-C. Gu, "Experimental studies of suppressing effectiveness on sloshing with two perforated floating plates," *International Journal of Naval Architecture and Ocean Engineering*, vol. 11, no. 1, pp. 285–293, 2019.
- [10] E. Botia-Vera et al., "Three SPH Novel Benchmark Test Cases for free surface flows," 2010.
- [11] Zhang, Y., Ma, S., Liao, K., & Duan, W. (2021). A numerical model for simulating two-phase flow with adaptive mesh refinement. *Computer Modeling in Engineering & Sciences*, 128(1), 43–64.

- [12] Sufyan, M., Ngo, L. C., & Choi, H. G. (2017). A dynamic adaptation method based on unstructured mesh for solving sloshing problems. *Ocean Engineering*, 129, 203–216.
- [13] Castillo, E., Cruchaga, M. A., Baiges, J., & Flores, J. (2018). An oil sloshing study: Adaptive Fixed-mesh analysis and comparison with experiments. *Computational Mechanics*, 63(5), 985–998.
- [14] Nema, P. K., & Kapil. (2019). Computational analysis of sloshing in 3-D rectangular tank under seismic excitation with and without baffle. *International Journal of Research in Engineering and Innovation*, 3(5), 330–338.